Int. J. Heat Mass Transfer. Vol. 26, No. 5, pp. 639–653, 1983
Printed in Great Britain

0017–9310/83/050639–15 $03.00/0
Pergamon Press Ltd.

A THEORETICAL STUDY OF LAMINAR MIXED CONVECTION FROM A HORIZONTAL CYLINDER IN A CROSS STREAM

H. M. BADR
Mechanical Engineering Department, University of Petroleum & Minerals, Box No. 322, Dhahran, Saudi Arabia

(*Received* 26 *June* 1982)

Abstract—The problem of laminar mixed convection from a horizontal isothermal cylinder is considered. The free stream direction is assumed to be horizontal and perpendicular to the cylinder axis. The study is based on the solution of the full Navier–Stokes and energy equations for 2-dim. flow of a Boussinesq fluid. The free stream is assumed to start impulsively from rest and the velocity and thermal boundary layers are developed in time until reaching steady conditions. The investigation covered the ranges of Reynolds number $1 < Re < 40$ and Grashof numbers up to $Gr = 5\,Re^2$ while keeping Prandtl number at a constant value of 0.7. Comparison of results with previous experimental correlations shows a good agreement. The streamline and isotherm patterns are plotted and different aspects of the phenomenon are discussed.

NOMENCLATURE

a,	cylinder radius;
c,	specific heat;
f_n, F_n,	functions defined in equation (14);
F_r, F_θ,	radial and transverse components of the body force;
g,	gravitational acceleration;
g_n, G_n,	functions defined in equation (14);
Gr,	Grashof number, $g\beta(T_s - T_\infty)(2a)^3/\nu^2$;
h, $\bar{h}$,	local and average heat transfer coefficients;
h_n, H_n,	functions defined in equation (14);
k,	thermal conductivity;
Nu, $\overline{Nu}$,	local and average Nusselt numbers;
p^*,	dimensionless pressure defined in equation (24);
Pe,	Péclet number, $Re\,Pr$;
Pr,	Prandtl number, $\mu c/k$;
$\dot{q}$,	rate of heat transfer per unit area;
r,	radial coordinate;
Re,	Reynolds number, $2aV/\nu$;
t,	dimensionless time;
T,	temperature;
v_r, v_θ,	radial and transverse components of velocity;
V,	uniform stream velocity.

Greek symbols

β,	coefficient of volumetric thermal expansion;
δ,	constant defined following equation (18);
ξ,	logarithmic radial coordinate, $\ln(r/a)$;
ρ,	density;
ν,	kinematic viscosity;
ϕ,	dimensionless temperature, $(T - T_\infty)/(T_s - T_\infty)$;
ψ,	dimensionless stream function, ψ'/aV;
θ,	angular coordinate;
ζ,	dimensionless vorticity, $\zeta' a/V$.

1. INTRODUCTION

HEAT transfer from a horizontal cylinder has been the subject of many experimental and theoretical investigations because of its numerous engineering applications. Although theoretical treatment of pure natural and pure forced convection from circular cylinders has been carried out successfully in the past [1–4], it seems that no theoretical study has been conducted to investigate the general case of combined forced and natural convection especially when the direction of the forced flow differs from that of natural convection. Most of the studies reported aim more or less to correlate the experimental data and make no attempt to solve the full Navier–Stokes and energy equations for such a basic and important problem. The only exception is the work by Nakai and Okazaki [5] which is limited to heat transfer regimes that are either dominated by forced or free convection. Their study was restricted to very small Reynolds, Re, and Grashof, Gr, numbers and yet was unsuccessful in tackling the problem of cross mixed convection when the natural convection is dominant.

Experimental investigation of mixed convection at low Reynolds number ($Re < 0.4$) was reported in the work by Collis and Williams [6] to evaluate the effect of free convection on the overall heat transfer rate from a hot wire. A good account of the work done on this problem prior to 1959 is to be found there. The first extensive study on combined convection from horizontal cylinders to air with special emphasis on hot wire anemometry is that by Hatton *et al.* [7]. In their work, heat transfer measurements were performed in the range of Re up to 45, Rayleigh number, Ra, up to 10, and for different flow directions. An experimental correlation based on vectorial summation of forced and natural convection was deduced. This correlation was not found to be successful in all flow directions. Gebhart and Pera [8] studied the same problem for various Prandtl numbers but restricted their study to very small Reynolds numbers. The phenomenon was

investigated experimentally in the high Re and Gr ranges (Re up to 5×10^3 and Gr up to 7×10^3) by Sharma and Sukhatme [9]. In their work, a criterion for transition from free to combined to forced convection is suggested. Mixed convection from a horizontal cylinder to water was studied by Fand and Keswani [10] and by Bennon and Incropera [11]. The influence of flow direction on combined heat convection from a horizontal cylinder to air was studied experimentally by Oosthuizen and Madan [12] but no general correlation was given.

The special case when the forced flow is vertically upward was studied experimentally by Oosthuizen and Madan [13] and by Jackson and Yen [14]. Theoretical treatment of the same problem was found in the work by Arcivos [15], Sparrow and Lee [16] and lately by Merkin [17] who studied the two cases of flow over hot and cold cylinders.

In this work, the problem of combined convection heat transfer from an isothermal circular cylinder placed with its axis horizontal and perpendicular to the free stream direction is considered. The full mass, momentum and energy conservation equations are solved simultaneously in the range of Reynolds number, based on free stream condition, of $1 < Re < 40$ while the Grashof number varied in the range $0 < Gr/Re^2 < 5$. The streamline and isotherm patterns were plotted and the results were compared with previous experimental correlations. Different aspects of the phenomenon were discussed.

2. GOVERNING EQUATIONS AND BOUNDARY CONDITIONS

In the problem considered, a circular heated cylinder is placed horizontally in a uniform stream with its axis perpendicular to the oncoming flow direction. The forced flow is assumed to be perpendicular to the direction of free convection. The cylinder has an isothermal surface with a constant temperature, T_s. The effect of temperature variation on fluid properties are considered negligible except for the body force term in the momentum equation (the Boussinesq approximation). The cylinder's end effects on the velocity and temperature fields are neglected and accordingly the flow is assumed 2-dim. Consider that the cylinder radius is a and the line $\theta = 0$ is the radius through the rearmost point on the cylinder surface. The velocity of the uniform stream is in the direction $\theta = 0$. Assuming time dependent flow in the (r', θ) plane, the three conservation principles can be expressed in the form of the vorticity, stream function and energy equations as

$$\frac{\partial \zeta'}{\partial t'} + v'_{r'}\frac{\partial \zeta'}{\partial r'} + \frac{v'_\theta}{r'}\frac{\partial \zeta'}{\partial \theta} = \nu \nabla^2 \zeta' - \left(\frac{1}{\rho}\right)\left(\frac{\partial F_\theta}{\partial r'} - \frac{1}{r'}\frac{F_{r'}}{\partial \theta} + \frac{F_\theta}{r'}\right), \quad (1)$$

$$\zeta' = \nabla^2 \psi', \quad (2)$$

$$\frac{\partial T}{\partial t'} + v'_{r'}\frac{\partial T}{\partial r'} + \frac{v'_\theta}{r'}\frac{\partial T}{\partial \theta} = \left(\frac{k}{\rho c}\right)\nabla^2 T, \quad (3)$$

where

$$\nabla^2 = \frac{\partial^2}{\partial r'^2} + \frac{1}{r'}\frac{\partial}{\partial r'} + \frac{1}{r'^2}\frac{\partial^2}{\partial \theta^2},$$

t' is the time, $v'_{r'}$ and v'_θ are the velocities in the r' and θ directions, T is the temperature, ρ is the density, ν is the kinematic viscosity, k is the thermal conductivity and c is the specific heat. $F_{r'}$ and F_θ represent the radial and transverse components of the body force and defined as

$$F_{r'} = \rho g \beta (T - T_\infty) \sin \theta,$$
$$F_\theta = \rho g \beta (T - T_\infty) \cos \theta \quad (4)$$

where g is the gravitational acceleration, β is the coefficient of thermal expansion and T_∞ is the fluid temperature far away from the cylinder. The vorticity ζ' and stream function ψ' are related to the velocity field by

$$\zeta' = -\frac{1}{r'}\left(r'\frac{\partial v'_\theta}{\partial r'} + v_\theta - \frac{\partial v'_{r'}}{\partial \theta}\right)$$

and (5)

$$v'_{r'} = \frac{1}{r'}\frac{\partial \psi'}{\partial \theta}, \quad v'_\theta = -\frac{\partial \psi'}{\partial r'}.$$

The equations are transformed to their non-dimensional form by introducing the following dimensionless quantities:

$$v_r = \frac{v'_{r'}}{V}, \quad v_\theta = \frac{v'_\theta}{V}, \quad r = \frac{r'}{a}, \quad t = t'\frac{V}{a}, \quad \psi = \frac{\psi'}{aV},$$

$$\zeta = \zeta'\frac{a}{V}, \quad \text{and} \quad \phi = (T - T_\infty)/(T_s - T_\infty)$$

where V is the velocity of the uniform stream. Using the above variables, equation (1)–(3) can now be written as

$$\frac{\partial \zeta}{\partial t} + v_r\frac{\partial \zeta}{\partial r} + \frac{v_\theta}{r}\frac{\partial \zeta}{\partial \theta} = \left(\frac{2}{Re}\right)\nabla^2 \zeta - \frac{Gr}{2Re^2}\left(\cos\theta\frac{\partial \phi}{\partial r} - \frac{\sin\theta}{r}\frac{\partial \phi}{\partial \theta}\right), \quad (6)$$

$$\zeta = \nabla^2 \psi, \quad (7)$$

$$\frac{\partial \phi}{\partial t} + v_r\frac{\partial \phi}{\partial r} + \frac{v_\theta}{r}\frac{\partial \phi}{\partial \theta} = \frac{2}{RePr}\nabla^2 \phi, \quad (8)$$

where

$$v_r = \left(\frac{1}{r}\right)\frac{\partial \psi}{\partial \theta}, \quad v_\theta = -\frac{\partial \psi}{\partial r},$$

$Re = \dfrac{2aV}{\nu}$ is the Reynolds number,

$Pr = \dfrac{\mu c}{k}$ is the Prandtl number, and

$Gr = \dfrac{g\beta(2a)^3(T_s - T_\infty)}{\nu^2}$ is the Grashof number.

The boundary conditions are

$$v_r = v_\theta = 0 \quad \text{and} \quad \phi = 1 \quad \text{at} \quad r = 1,$$
$$v_r \to \cos\theta,\ v_\theta \to -\sin\theta,\ \zeta \to 0 \qquad (9)$$
$$\text{and } \phi \to 0 \text{ as } r \to \infty.$$

These conditions are based on the no-slip and isothermal conditions on the cylinder surface together with the free stream conditions away from it.

3. THE METHOD OF SOLUTION

In this work the steady solution of the governing equations was obtained through studying the time development of the velocity and thermal boundary layers around the cylinder starting from certain initial conditions. This is achieved through integrating the governing equations in time until reaching the fully developed velocity and temperature fields. In principle, the same approach has been used by many investigators [18, 19]. It is assumed that initially the cylinder is placed in a fluid at rest with no temperature difference ($T_s = T_\infty$). The motion of the uniform stream is assumed to start impulsively from rest with velocity V and after a small time t^* the cylinder is heated instantaneously to the constant surface temperature T_s. In the first phase of the motion the velocity boundary layer develops partially with no body force effect since the temperature is the same everywhere. In the second phase the velocity and thermal layers develop simultaneously with time until reaching the steady conditions.

The method of solution is a generalization of the method developed by Badr and Dennis [20] to include the buoyancy term in the vorticity equation and to solve the energy equation simultaneously for obtaining the temperature field. In this method the modified polar coordinates (ξ, θ) are used, where $\xi = \ln(r/a)$ and accordingly the governing equations (6)–(8) are transformed to

$$e^{2\xi}\frac{\partial\zeta}{\partial t} = \frac{2}{Re}\left(\frac{\partial^2\zeta}{\partial\xi^2} + \frac{\partial^2\zeta}{\partial\theta^2}\right) - \frac{\partial\psi}{\partial\theta}\frac{\partial\zeta}{\partial\xi} + \frac{\partial\psi}{\partial\xi}\frac{\partial\zeta}{\partial\theta} - e^{\xi}\frac{Gr}{2Re^2}\left[\cos\theta\frac{\partial\phi}{\partial\xi} - \sin\theta\frac{\partial\phi}{\partial\theta}\right], \qquad (10)$$

$$e^{2\xi}\zeta = \frac{\partial^2\psi}{\partial\xi^2} + \frac{\partial^2\psi}{\partial\theta^2}, \qquad (11)$$

$$e^{2\xi}\frac{\partial\phi}{\partial t} = \frac{2}{RePr}\left(\frac{\partial^2\phi}{\partial\xi^2} + \frac{\partial^2\phi}{\partial\theta^2}\right) - \frac{\partial\psi}{\partial\theta}\frac{\partial\phi}{\partial\xi} + \frac{\partial\psi}{\partial\xi}\frac{\partial\phi}{\partial\theta} \qquad (12)$$

where

$$v_r = e^{-\xi}\frac{\partial\psi}{\partial\theta}$$

and

$$v_\theta = -e^{-\xi}\frac{\partial\psi}{\partial\xi}$$

and the boundary conditions given in equation (9) are transformed to

$$\psi = \frac{\partial\psi}{\partial\xi} = 0 \quad \text{and} \quad \phi = 1 \quad \text{at} \quad \xi = 0,$$
$$e^{-\xi}\frac{\partial\psi}{\partial\theta} \to \cos\theta,\ e^{-\xi}\frac{\partial\psi}{\partial\xi} \to \sin\theta,\ \zeta \to 0 \qquad (13)$$
$$\text{and} \quad \phi \to 0 \quad \text{as} \quad \xi \to \infty.$$

The method of series truncation developed by Badr and Dennis [20] and applied to study the asymmetrical flow field around a rotating cylinder was adopted for tackling the present problem. The asymmetry in the previous problem was due to the cylinder rotation. The cause of asymmetry in the present problem is the effect of the body forces. The dimensionless stream function ψ, vorticity ζ and temperature ϕ are expressed in Fourier series as

$$\psi = \tfrac{1}{2}F_0(\xi,t) + \sum_{n=1}^{N} f_n(\xi,t)\sin n\theta + F_n(\xi,t)\cos n\theta,$$
$$\zeta = \tfrac{1}{2}G_0(\xi,t) + \sum_{n=1}^{N} g_n(\xi,t)\sin n\theta + G_n(\xi,t)\cos n\theta,$$
$$\phi = \tfrac{1}{2}H_0(\xi,t) + \sum_{n=1}^{N} h_n(\xi,t)\sin n\theta + H_n(\xi,t)\cos n\theta. \qquad (14)$$

Substituting from equation (14) in equation (11), and by using simple mathematical analysis, one obtains

$$\frac{\partial^2 F_0}{\partial\xi^2} = e^{2\xi}G_0, \qquad (15a)$$

$$\frac{\partial^2 F_n}{\partial\xi^2} - n^2F_n = e^{2\xi}G_n, \qquad (15b)$$

$$\frac{\partial^2 f_n}{\partial\xi^2} - n^2 f_n = e^{2\xi}g_n \qquad (15c)$$

where

$$f_n = f_n(\xi,t),\quad g_n = g_n(\xi,t),\ldots,\text{etc.}$$

Similarly, using equation (14) together with equation (10), gives the following differential equations for G_0, g_n, and G_n:

$$e^{2\xi}\frac{\partial G_0}{\partial t} = \left(\frac{2}{Re}\right)\frac{\partial^2 G_0}{\partial\xi^2} + S_0, \qquad (16a)$$

$$2e^{2\xi}\frac{\partial g_n}{\partial t} = \left(\frac{4}{Re}\right)\left(\frac{\partial^2 g_n}{\partial\xi^2} - n^2 g_n\right) + nF_n\frac{\partial G_0}{\partial\xi} - nG_n\frac{\partial F_0}{\partial\xi} + S_{n1}, \qquad (16b)$$

$$2e^{2\xi}\frac{\partial G_n}{\partial t} = \left(\frac{4}{Re}\right)\left(\frac{\partial^2 G_n}{\partial\xi^2} - n^2 G_n\right) - nf_n\frac{\partial G_0}{\partial\xi} + ng_n\frac{\partial F_0}{\partial\xi} + S_{n2} \qquad (16c)$$

where the functions S_0, S_{n1}, and S_{n2} are defined in the Appendix. Finally, by using equation (14) together with

equation (12), we obtain

$$e^{2\xi}\frac{\partial H_0}{\partial t} = \left(\frac{2}{Pe}\right)\frac{\partial^2 H_0}{\partial \xi^2} + Z_0, \tag{17a}$$

$$2e^{2\xi}\frac{\partial h_n}{\partial t} = \left(\frac{4}{Pe}\right)\left(\frac{\partial^2 h_n}{\partial \xi^2} - n^2 h_n\right) + nF_n\frac{\partial H_0}{\partial \xi} - nH_n\frac{\partial F_0}{\partial \xi} + Z_{n1}, \tag{17b}$$

$$2e^{2\xi}\frac{\partial H_n}{\partial t} = \left(\frac{4}{Pe}\right)\left(\frac{\partial^2 H_n}{\partial \xi^2} - n^2 H_n\right) - nf_n\frac{\partial H_0}{\partial \xi} + nh_n\frac{\partial F_0}{\partial \xi} + Z_{n2} \tag{17c}$$

where Pe is the Péclet number ($Pe = RePr$) and the functions Z_0, Z_{n1}, and Z_{n2} are defined in the Appendix. It should be mentioned that $S_0, S_{n1}, S_{n2}, Z_0, Z_{n1}$, and Z_{n2} are all functions of ξ and t.

The boundary conditions for all the functions given in equations (15)–(17) are deduced from equations (13) and (14) and can be written as

$$\left.\begin{aligned} &F_0 = f_n = F_n = h_n = H_n = 0 \\ &\frac{\partial F_0}{\partial \xi} = \frac{\partial f_n}{\partial \xi} = \frac{\partial F_n}{\partial \xi} = 0 \text{ and } H_0 = 2 \end{aligned}\right\} \text{ at } \xi = 0, \tag{18a}$$

$$\left.\begin{aligned} &\frac{\partial F_0}{\partial \xi} \to 0, \quad \frac{\partial F_n}{\partial \xi} \to 0, \quad \frac{\partial f_n}{\partial \xi} \to \delta_n e^{\xi} \\ &F_0, F_n, G_0, g_n, G_n, H_0, h_n \text{ and } H_n \to 0 \\ &f_n \to \delta_n e^{\xi} \end{aligned}\right\} \text{ as } \xi \to \infty, \tag{18b}$$

where

$$\delta_n = \begin{cases} 1 \text{ for } n = 1, \\ 0 \text{ for } n \neq 1. \end{cases}$$

By integrating both sides of equation (15a) with respect to ξ from $\xi = 0$ to $\xi = \infty$, and applying the boundary conditions given in equations (18), we obtain the following integral conditions:

$$\int_0^\infty e^{2\xi} G_0 \, d\xi = 0. \tag{19a}$$

Similarly we deduce from equations (15b) and (15c) the following two integral conditions for g_n and G_n:

$$\int_0^\infty e^{(2-n)\xi} g_n \, d\xi = 2\delta_n, \tag{19b}$$

$$\int_0^\infty e^{(2-n)\xi} G_n \, d\xi = 0. \tag{19c}$$

It is important here to know that the integral condition given in equation (19a) is necessary to ensure the continuity of pressure around the cylinder surface.

In the first phase of the motion the uniform stream starts impulsively from rest with no cylinder heating ($\phi = 0$ everywhere). In this phase the body force term in equation (10) vanishes and the streamline pattern is symmetrical and accordingly the cosine terms are omitted from the Fourier series expansion [equation (14)] since ψ and ζ are antisymmetric functions about the line $\theta = 0$. Since the boundary layer thickness is very small after the beginning of the fluid motion, the coordinate ξ was replaced by x where $\xi = 2(2t/Re)^{1/2}x$. The solution procedure in this phase is exactly the same as that used by Badr and Dennis [20] for the special case of no cylinder rotation. The integration process ended in this phase when $\xi = x$ which corresponds to time $t^* = Re/8$. At that time the boundary layer becomes thick enough to switch to the original coordinate system (ξ, θ).

In the second phase of the motion, the cylinder surface temperature is raised instantaneously to T_s and the thermal boundary layer is now allowed to develop simultaneously with the velocity boundary layer until reaching the final steady conditions. In this phase the velocity and temperature fields are asymmetric due to the effect of the body forces and accordingly the full equations (10)–(12) are considered. The initial conditions for this phase are exactly the same as the final solution obtained from the first phase at time $t = t^*$ [i.e. $g_n(\xi, t^*)$ and $f_n(\xi, t^*)$] with the rest of the functions F_0, F_n, G_0, and G_n set equal to zero. The instantaneous heating at $t = t^*$ will result in $\phi = 0$ everywhere except on the cylinder surface where $\phi = 1$. This corresponds to the following initial conditions:

$$H_0(\xi, t^*) = \begin{cases} 2 \text{ at } \xi = 0, \\ 0 \text{ for } \xi > 0 \end{cases} \tag{20}$$

and

$$h_n(\xi, t^*) = H_n(\xi, t^*) = 0.$$

The time development of the velocity and temperature fields is obtained by advancing the solution of ψ, ζ, and ϕ in time. This is achieved by integrating equations (15)–(17) numerically. A brief description of the numerical method is given in the following section.

4. THE NUMERICAL METHOD

The solutions of ψ, ζ, and ϕ are advanced in time by solving the three sets of equations (15)–(17) using a Crank–Nicolson finite-difference scheme. At a typical time t, it is required to obtain the functions $G_0(\xi, t)$, $g_n(\xi, t)$, and $G_n(\xi, t)$ to determine the vorticity distribution, the functions $F_0(\xi, t)$, $f_n(\xi, t)$, and $F_n(\xi, t)$ to determine the stream function and the functions $H_0(\xi, t)$, $h_n(\xi, t)$, and $H_n(\xi, t)$ to determine the temperature distribution provided that all these functions are known at time $(t - \Delta t)$, where Δt is the time increment. In the following the solution procedure for equation (16b) is described in some detail and similar procedures are used for solving equations (16a) and (16c).

Equation (16b) can be written as

$$\frac{\partial g_n}{\partial t} = q_n(\xi, t) \tag{21}$$

where

$$q_n(\xi,t)=\frac{e^{-2\xi}}{2}\left[\frac{4}{Re}\left(\frac{\partial^2 g_n}{\partial\xi^2}-n^2 g_n\right)+nF_n\frac{\partial G_0}{\partial\xi}-nG_n\frac{\partial F_0}{\partial\xi}+S_{n1}\right]. \quad (22)$$

The Crank–Nicolson finite-difference approximation of equation (21) results in

$$\frac{1}{\Delta t}[g_n(\xi,t)-g_n(\xi,t-\Delta t)]=\tfrac{1}{2}[q_n(\xi,t)+q_n(\xi,t-\Delta t)]. \quad (23)$$

Using central differences for all derivatives in equation (22) and substituting in equation (23) and rearranging, one obtains

$$A(\xi)g_n(\xi-\Delta\xi,t)+B(\xi)g_n(\xi,t)+C(\xi)g_n(\xi+\Delta\xi,t)=D_n(\xi,t-\Delta t)+E_n(\xi,t) \quad (24)$$

where $\Delta\xi$ is the step size in ξ, A, B, and C are easily identifiable functions in ξ that can be calculated at each mesh point, $D_n(\xi,t-\Delta t)$ is a completely known function, and $E_n(\xi,t)$ is a function that depends on the solution at time t.

In theory, equation (16b) should be integrated in the region from $\xi=0$ to $\xi=\infty$. However, since the problem is solved numerically the conditions at ∞ are applied at $\xi=\xi_m$ where ξ_m defines the distance away from the cylinder at which ζ and ϕ have negligibly small values. In the solution ξ_m could have a value up to 10 which corresponds to a distance away from the cylinder as far as e^{10} times its radius.

Equation (24), when applied at every mesh point in the range from $\xi=\Delta\xi$ to $\xi=\xi_m$ will result in a set of algebraic equations that forms a tridiagonal matrix problem. This set of equations are solved for every value of n between 1 and N. The difficulty in solving this matrix problem is that the RHS of equation (24) is not completely defined since the term $E_n(\xi,t)$ depends on the required solution at time t. To overcome this difficulty, an iterative process was used in which the unknown functions $E_n(\xi,t)$ are assumed initially to be the same as $E_n(\xi,t-\Delta t)$ and then corrected according to the most recent available values. The iterative process stopped when the difference in the solution of $g_n(\xi,t)$ between two successive iterations is within a certain limit, i.e.

$$|g_n^{(m+1)}(\xi,t)-g_n^{(m)}(\xi,t)|<10^{-6} \quad (25)$$

where the superscript m denotes the iteration number. Equation (24) could not be applied on the cylinder surface due to the difficulties in calculating the derivatives at $\xi=0$. After solving the matrix problem and obtaining $g_n(\xi,t)$ in the range $\Delta\xi\leqslant\xi\leqslant\xi_m$ the integral condition (19b) was utilized to determine $g_n(0,t)$.

Having obtained a better approximation for $G_0(\xi,t)$, $g_n(\xi,t)$, and $G_n(\xi,t)$ the next step is to solve equation (15) for $F_0(\xi,t)$, $f_n(\xi,t)$, and $F_n(\xi,t)$. A direct solution of equation (15a) was obtained using a central finite-difference scheme. Equations (15b) and (15c) were solved using a step-by-step integration scheme similar to that used by Dennis and Chang [21]. A straightforward finite-difference solution for those equations resulted in an extremely unstable solution especially for large values of n. The solution procedure for equation (17) is similar to that used for equation (15) except that the boundary values of H_0, h_n, and H_n at $\xi=0$ are completely known and there are no integral conditions. The solution of the three sets of equations (15)–(17) is repeated until a convergence criteria similar to that given in equation (25) is achieved for all functions.

Following the start of the second phase of the motion the thermal boundary layer thickness is very small and the derivative $\partial H_0/\partial\xi$ is very large near the solid boundary. To obtain a reasonably accurate solution a small time step $\Delta t=10^{-2}$ is considered for the first 10 time steps and then Δt increased to 0.05. The space step $\Delta\xi$ was considered to be 0.1 for all cases during the second phase of the motion. Since the boundary layer thickness increases with time the value of ξ_m is also set to match this behavior. That is achieved by considering the value of ξ_m to satisfy the following criteria:

$$|\zeta(\xi_m,\theta,t)|<\varepsilon \quad \text{and} \quad \phi(\xi_m,\theta,t)<\varepsilon$$

where ε is a very small number.

The number of terms N in the Fourier series was 2 at the beginning of the first phase of the motion. This number is allowed to increase with time. One more term is added when the last non-zero term [either $g_N(0,t)$ or $G_N(0,t)$] reaches the value of 10^{-4}. The same criterion applies to the second phase of motion.

5. ACCURACY OF THE METHOD

The accuracy of the present theory, as well as the numerical technique, were verified by studying the special case of forced convection from a circular cylinder and comparing results with the theoretical and experimental data found in the literature. To be able to compare results let us introduce the local and average Nusselt numbers Nu and $\overline{Nu}$ such that

$$Nu=2ah/k, \quad (26a)$$

$$\overline{Nu}=2a\bar{h}/k \quad (26b)$$

where h and $\bar{h}$ are the local and overall heat transfer coefficients defined as

$$h=\dot{q}/(T_s-T_\infty),\quad \dot{q}=k\left(\frac{\partial T}{\partial r'}\right)_{r'=a}$$

and

$$\bar{h}=\frac{1}{2\pi}\int_0^{2\pi}h\,d\theta \quad (26c)$$

where $\dot{q}$ is the rate of heat transfer per unit area. From the above definitions one can deduce

$$Nu = -2\left(\frac{\partial\phi}{\partial\xi}\right)_{\xi=0} = -2\left[\frac{1}{2}\frac{\partial H_0}{\partial\xi} + \sum_{n=1}^{N}\left(\frac{\partial h_n}{\partial\xi}\sin n\theta + \frac{\partial H_n}{\partial\xi}\cos n\theta\right)\right]_{\xi=0} \quad (27a)$$

and

$$\overline{Nu} = -\left(\frac{\partial H_0}{\partial\xi}\right)_{\xi=0}. \quad (27b)$$

Figure 1 shows a comparison between the result obtained from the present work for $Pr = 0.73$, $1 < Re < 40$, and $Gr = 0$ and the theoretical results obtained by Dennis *et al.* [1] and the experimental correlations predicted by Collis and Williams [6] and by Hatton *et al.* [7] for the same case. Small differences (less than 2.5%) were found between $\overline{Nu}$ predicted by the present theory and the theoretical results [1]. A comparison with the experimental correlation by Collis and Williams [6] shows small differences at low Reynolds numbers. The difference increases with the increasing of Re, reaching 10% at $Re = 40$. On the other hand, the present results compare well with the experimental formula of Hatton *et al.* [7] at high Re values, but percentage differences increase as Re decreases. The difference between the present results and experimental correlations are believed to be due to the following reasons:

(1) In theory, the cylinder end effects were neglected and accordingly the flow is considered 2-dim. over the entire length of the cylinder.

(2) The fluid properties are considered invariant and no temperature correction factor was applied.

(3) The uncertainty in the experimental measurements (for example, in Hatton's work the maximum uncertainty in the values of $\overline{Nu}$ were $\pm 5\%$ for the case of flow over a wire).

6. RESULTS AND DISCUSSION

It has been known that the coefficient of heat transfer in a particular mixed convection problem depends on Reynolds number, Re, Grashof number, Gr, Prandtl number, Pr, in addition to direction of the forced flow. These parameters can also be deduced from the governing equations (6)–(8). Equation (6) shows also that the difference between the velocity field in case of mixed convection and that of forced convection depends mainly on the parameter Gr/Re^2 which represent the ratio between buoyant and interial forces.

The mathematical model introduced in Section (3) was used to predict the time development of the velocity and temperature boundary layers around the cylinder. For each of the cases considered, the steady state was achieved after a certain time from the start of the motion. This time varied from one case to another, the maximum time value needed being $t = 20$. The variation of the average Nusselt number $\overline{Nu}$ with time following the sudden rise in the cylinders' temperature is shown in Fig. 2 when $Re = 5$ for the cases of forced and mixed convection regimes. $\overline{Nu}$ has its maximum value immediately after the cylinder is heated since the thermal boundary layer thickness is very small. With the increase of time this thermal boundary layer thickens and $\overline{Nu}$ decreases accordingly.

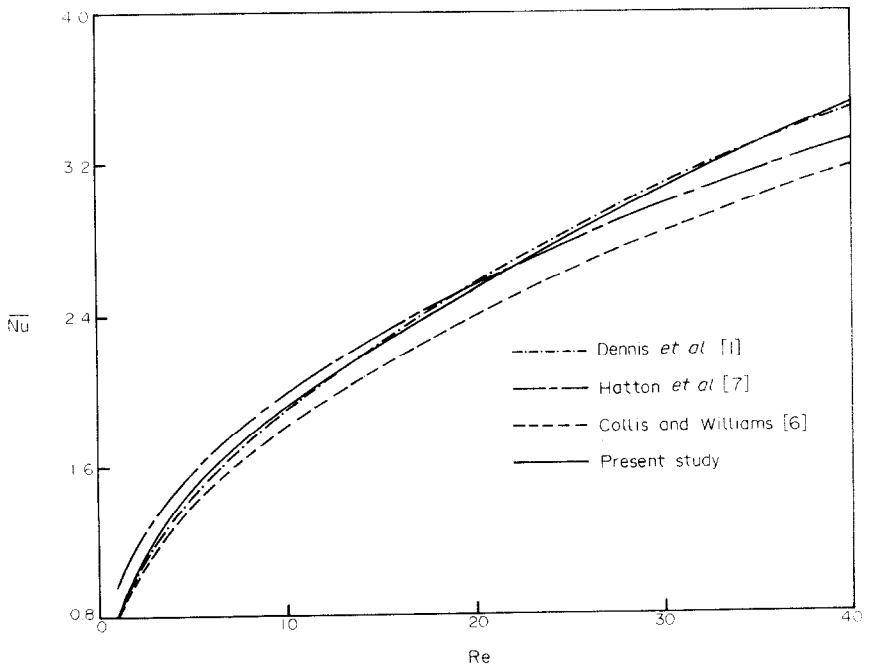

FIG. 1. Comparison between $\overline{Nu}$ obtained from the present work and previous experimental and theoretical results for the special case of forced convection.

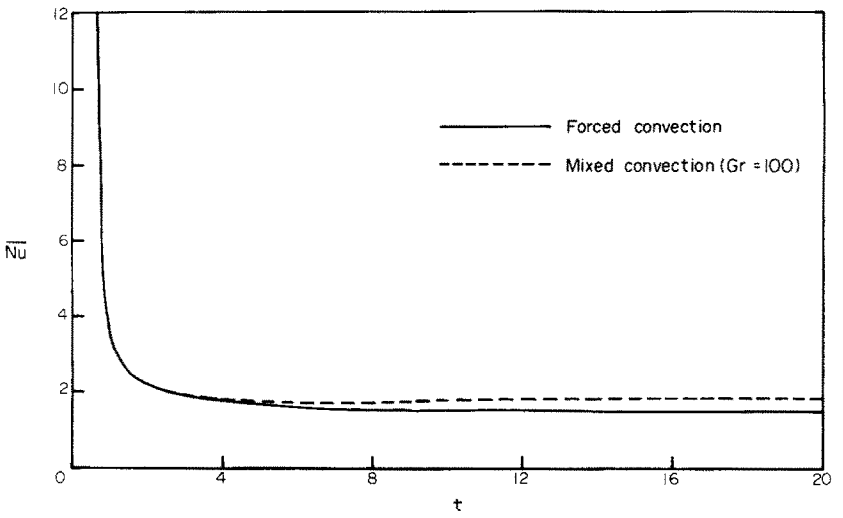

FIG. 2. Variation of $\overline{Nu}$ with time after the sudden heating of the cylinder, $Re = 5$.

The ratio Gr/Re^2 was found to have a great influence on the velocity and thermal boundary layers. Figures 3(a) and (b) show the variation of vorticity ζ on the cylinder surface for the cases when $Re = 5$ and 20 and for different values of Gr. It is clear from these figures that the surface vorticity, and accordingly the velocity gradient at the surface, increase significantly with the increase of Gr. This is mainly because the buoyant forces are aiding the flow around most of the cylinder surface. This effect results in reducing the pressure and creating regions of suction. To examine the pressure distribution let us introduce the dimensionless pressure p^* defined as

$$p_\theta^* = (p_\theta - p_\pi)/\tfrac{1}{2}\rho V^2. \tag{28}$$

By integrating the transverse component of the Navier–Stokes equations, one can prove that p^* is related to the vorticity field by

$$p^* = \frac{4}{Re}\int_\theta^\pi \left(\frac{\partial\zeta}{\partial\xi}\right)_{\xi=0} \mathrm{d}\theta + \frac{Gr}{Re^2}\sin\theta. \tag{29}$$

The pressure variation around the cylinder surface for the cases of $Re = 5$ and 20 are shown in Figs. 4(a) and (b). From these figures it is clear that increasing Gr results in a considerable pressure reduction around the cylinder. The zone of maximum suction occurred in all the cases considered between $\theta = 260$ and 310°. However, the exact location depends on Re as well as Gr. In their analysis of the problem of free convection with slight cross forced convection, Nakai and Okazaki [5] predicted that the effect of secondary suction flow extends to large distances away from the cylinder. This is the main reason for which their similarity solution could not be employed accurately since the uniform

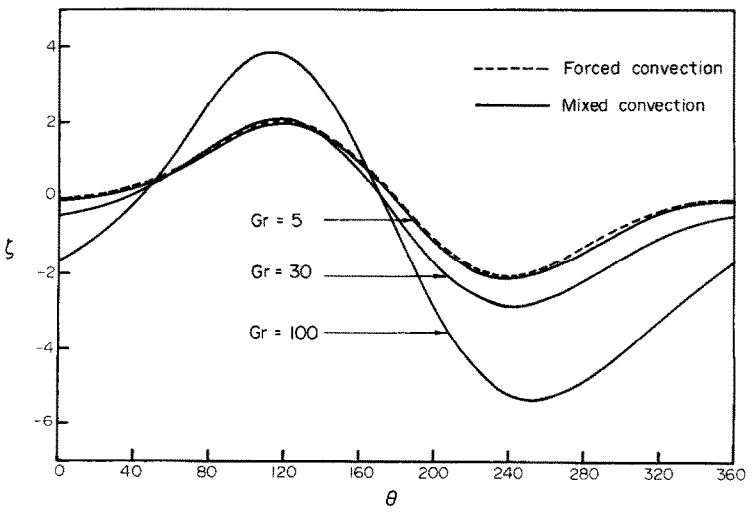

FIG. 3(a). Vorticity distribution on the cylinder surface, $Re = 5$.

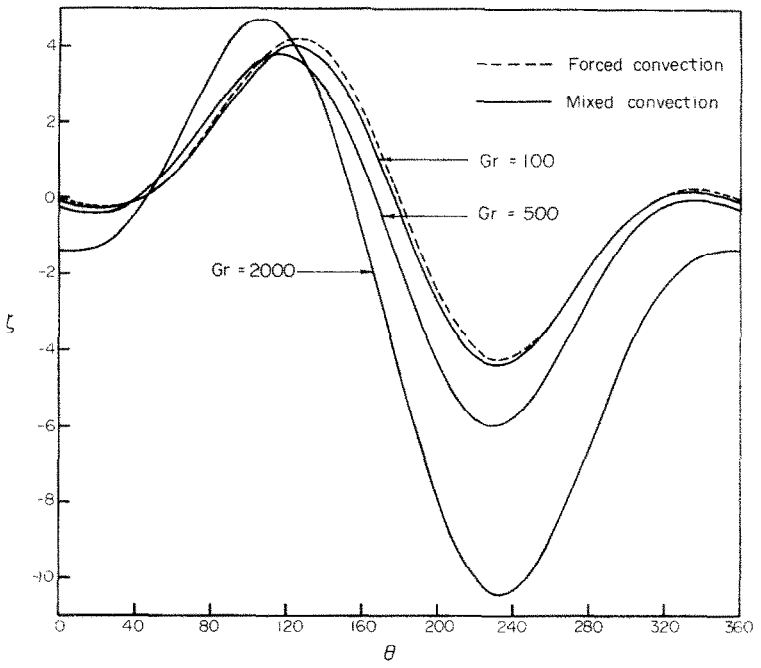

FIG. 3(b). Vorticity distribution on the cylinder surface, $Re = 20$.

flow has been disturbed upstream and downstream of the cylinder. The effect of suction on the streamline pattern is shown in Figs. 5 and 6 for the cases of $Re = 5$ and $Re = 20$ and for different values of Gr. The streamlines upstream of the cylinder have a downward slope towards the point of minimum pressure. The reverse flow in the wake of the cylinder is strongly influenced by the ratio Gr/Re^2. It was found that at large values of Gr/Re^2 no reverse flow takes place in the wake and the vortices completely disappear.

The variation of the local Nusselt number Nu around the cylinder surface is shown in Figs. 7(a) and (b) for the cases of $Re = 5$ and $Re = 20$, respectively. For forced convection regime ($Gr = 0$) Nu is maximum at $\theta = 180°$ and minimum at $\theta = 0$. With the increase of Gr the maximum value of Nu continues to occur near 180°.

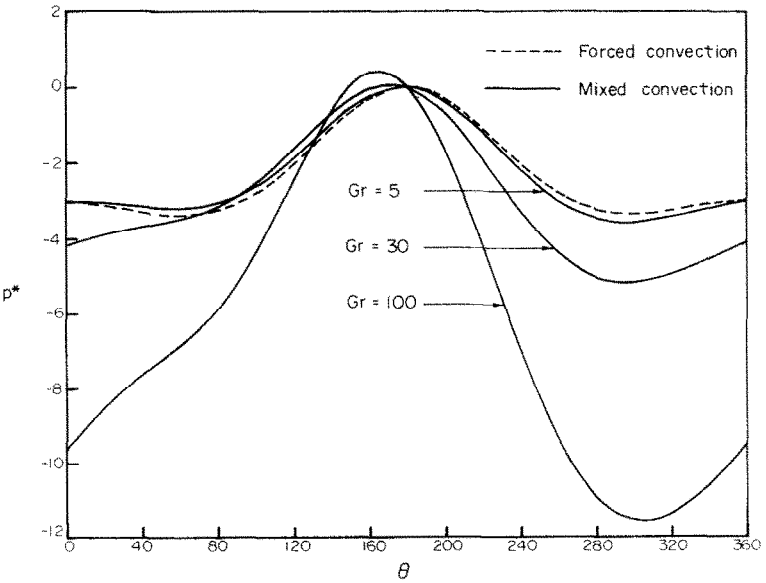

FIG. 4(a). Pressure distribution around the cylinder surface, $Re = 5$.

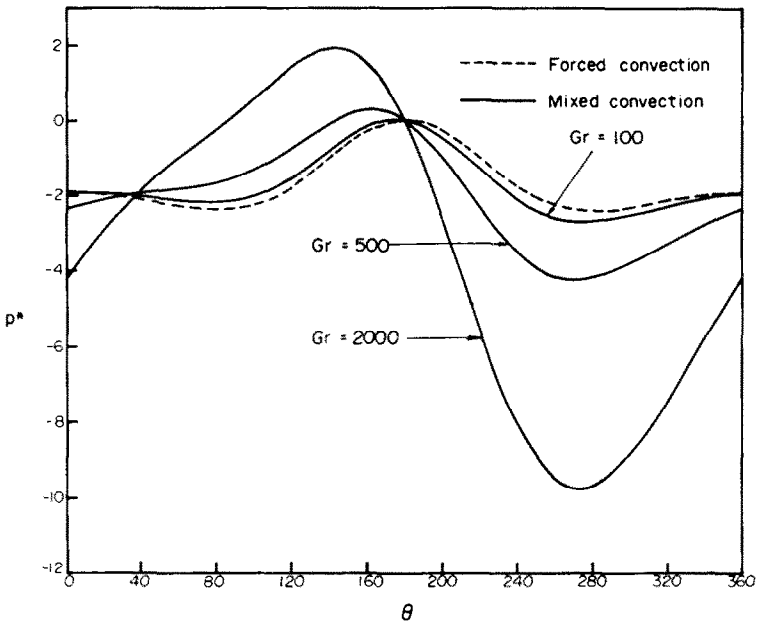

FIG. 4(b). Pressure distribution around the cylinder surface, $Re = 20$.

however, the point of minimum Nu moves upward towards $\theta = 90°$. The exact location of that point depends on Gr/Re^2. It was also found that Nu over most of the cylinder surface, and accordingly $\overline{Nu}$, increase with the increase of Grashof number. The results obtained from the present theory for $\overline{Nu}$ were compared with the following experimental correlation deduced by Hatton *et al.* [7]:

$$\overline{Nu}(T_f/T_\infty)^{-0.154} = 0.384 + 0.581\, Re_{eff}^{0.439} \quad (30)$$

where $(T_f/T_\infty)^{-0.154}$ is a temperature correction factor and Re_{eff} is the effective Reynolds number defined for the case of cross flow as

$$Re_{eff} = Re_f[1 + 1.06\, Ra^{0.836}/Re_f^2]^{1/2} \quad (31)$$

where Ra is the Rayleigh number and Re_f is the Reynolds number of the forced flow.

Figure 8 shows a comparison between Hatton's correlation and the present results which were plotted on the same coordinates assuming no temperature correction for both cases. Although in Hatton's experiments the range of Ra covered was up to 10, it seems that the agreement with the theoretical results is in general very satisfactory. The difference between the two at high Re_{eff} is within 3%. The percentage difference is higher at small Re_{eff}, but Hatton's correlation differs by the same amount from that of Collis and Williams for the case of forced convection. The numerical values of $\overline{Nu}$ for all the cases considered are listed in Table 1.

Figure 9 shows the effect of natural convection on the relative increase of the average Nusselt number at different values of Re. In the range of Re and Gr considered, it was found that the increase in $\overline{Nu}$ did not exceed 4% when $Gr/(Re^2) < 1.0$. Another interesting phenomenon that can be seen clearly in the case of $Re = 20$, that is for small values of $Gr[Gr/(Re^2) \simeq 0.2]$. The average Nusselt number decreased slightly in comparison with the pure forced convection value at the same Re. The same phenomenon was detected experimentally by Hatton *et al.* [7] who found that some of the measured $\overline{Nu}$ for mixed convection regimes are less than the corresponding forced convection values.

The effect of Grashof number on the thermal boundary layer is presented by plotting the lines of equal temperature (isotherms). Figures 10 and 11 show the isotherm patterns for the cases of $Re = 5$ and $Re = 20$ and for different values of Gr in each case. When Gr is small the temperature field is almost

Table 1. Values of the average Nusselt number $\overline{Nu}$ for the case of $Pr = 0.7$

Re	Gr	$\overline{Nu}$	Re	Gr	$\overline{Nu}$
1	0	0.800	20	0	2.54
1	1	0.865	20	100	2.52
1	2	0.902	20	500	2.65
1	3	0.930	20	1000	2.85
1	4	0.955	20	1600	3.02
			20	2000	3.10
5	0	1.45	40	0	3.48
5	5	1.45	40	400	3.49
5	30	1.51	40	2000	3.60
5	60	1.65	40	3200	3.76
5	100	1.82	40	6400	4.17
5	125	1.89			

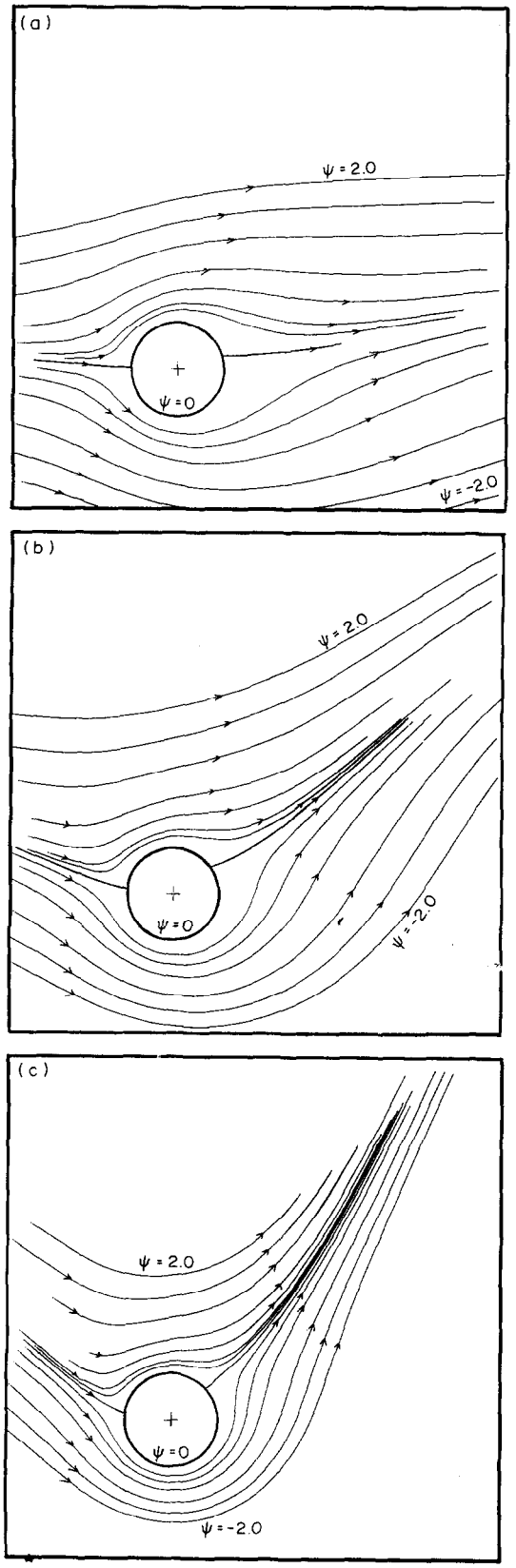

FIG. 5. Streamline patterns for $Re = 5$. (a) $Gr = 5$. (b) $Gr = 30$. (c) $Gr = 100$. (Streamlines plotted are $\psi = -2.0, -1.5, -1.0, -0.5, -0.25, -0.1, 0, 0.1, 0.25, 0.5, 1.0, 1.5$, and 2.0).

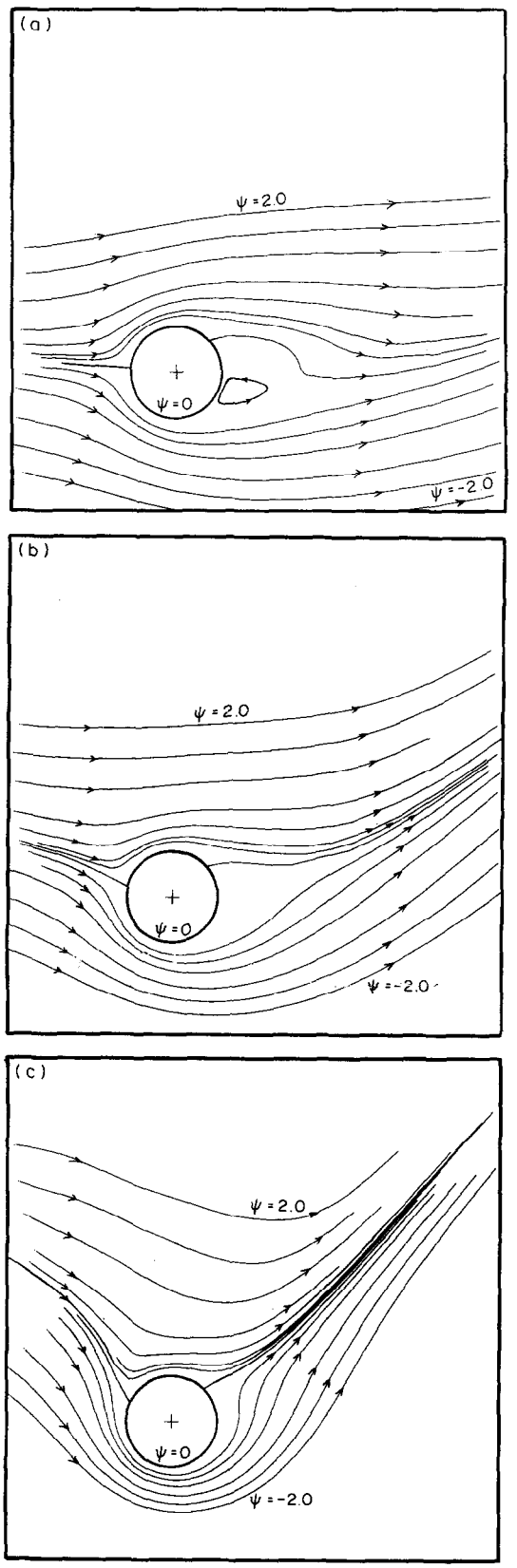

FIG. 6. Streamline patterns for $Re = 20$. (a) $Gr = 100$. (b) $Gr = 500$. (c) $Gr = 2000$. (Streamlines plotted are $\psi = -2.0, -1.5, -1.0, -0.5, -0.25, -0.1, 0, 0.1, 0.25, 0.5,$

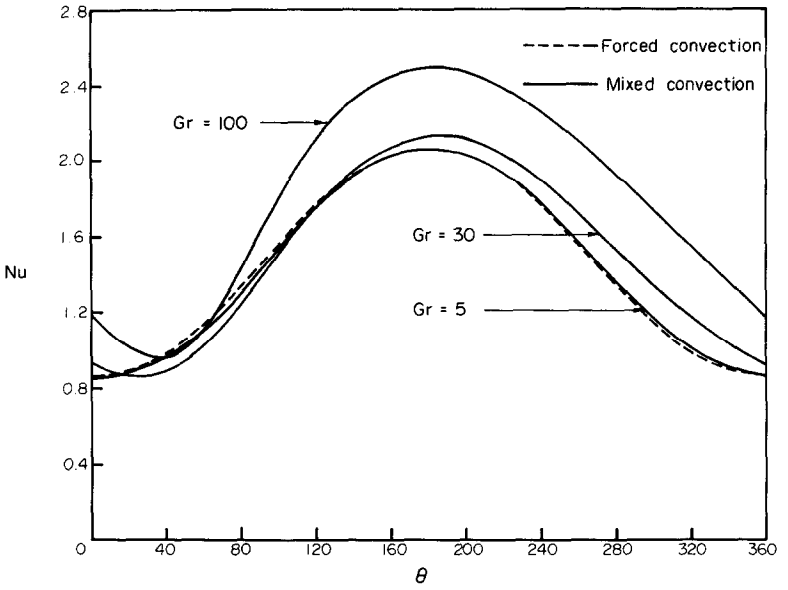

FIG. 7(a). Variation of the local Nusselt number around the cylinder surface, $Re = 5$.

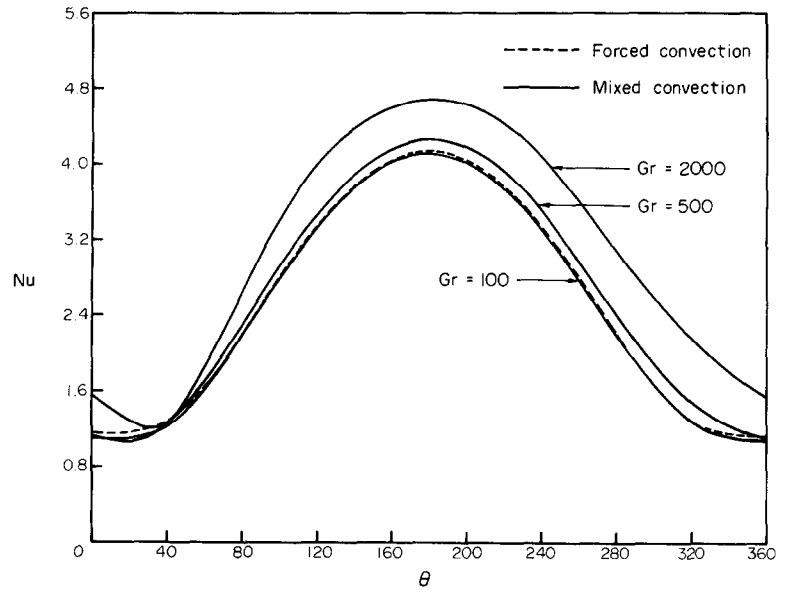

FIG. 7(b). Variation of the local Nusselt number around the cylinder surface, $Re = 20$.

symmetrical about the line $\theta = 0$. With the increase of Gr the point of plume separation moves upward and the isotherm pattern changes accordingly.

7. CONCLUSIONS

The problem of cross mixed convection from a horizontal circular cylinder is investigated in the range of Reynolds number $1 < Re < 40$ and Grashof numbers up to $Gr/(Re^2) = 5$ while keeping Prandtl number at $Pr = 0.7$. The study is based on the solution of the full Navier–Stokes and energy equations. A mathematical model was constructed and then tested by studying the problem of forced convection in the same range of Re. By comparing results with previous theoretical and experimental data a good agreement was found. The method was then applied successfully to study the main problem of cross mixed convection. The details of the steady velocity and thermal boundary layers were obtained and accordingly the variation of vorticity, pressure, and local Nusselt number around

the cylinder surface were plotted for various cases. The resulting values of the average Nusselt number were tabulated and compared with Hatton's experimental correlation where a good agreement was found. The streamline and isotherm patterns were plotted to show some of the details of the velocity and temperature fields.

Acknowledgement—The author wishes to acknowledge the support received from the University of Petroleum and Minerals, Dhahran, Saudi Arabia.

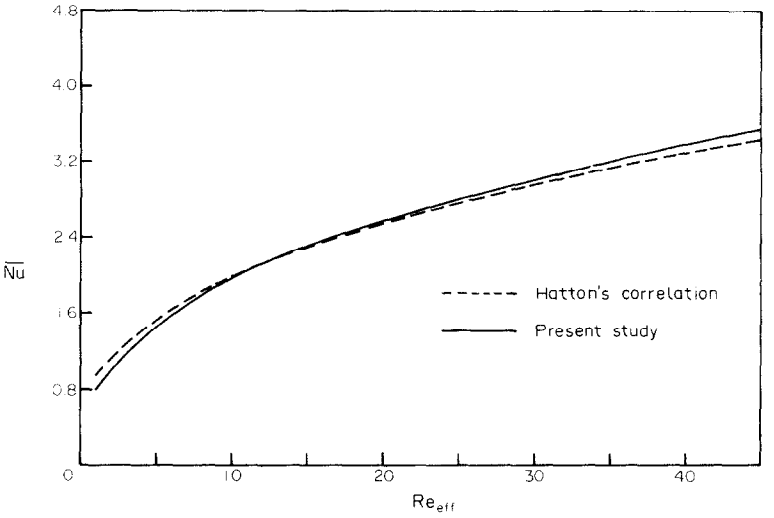

FIG. 8. Comparison between the values of $\overline{Nu}$ obtained from the present study and the experimental correlation by Hatton *et al.* [7].

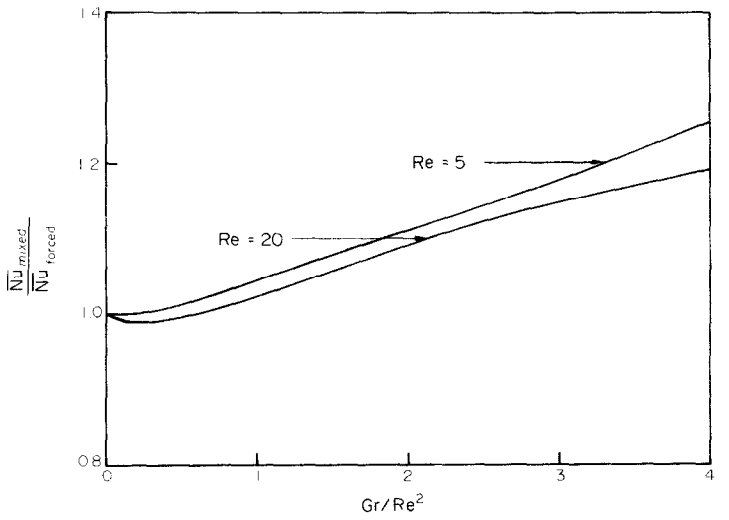

FIG. 9. Effect of the ratio Gr/Re^2 on the relative increase of the average Nusselt number for $Re = 5$ and 20.

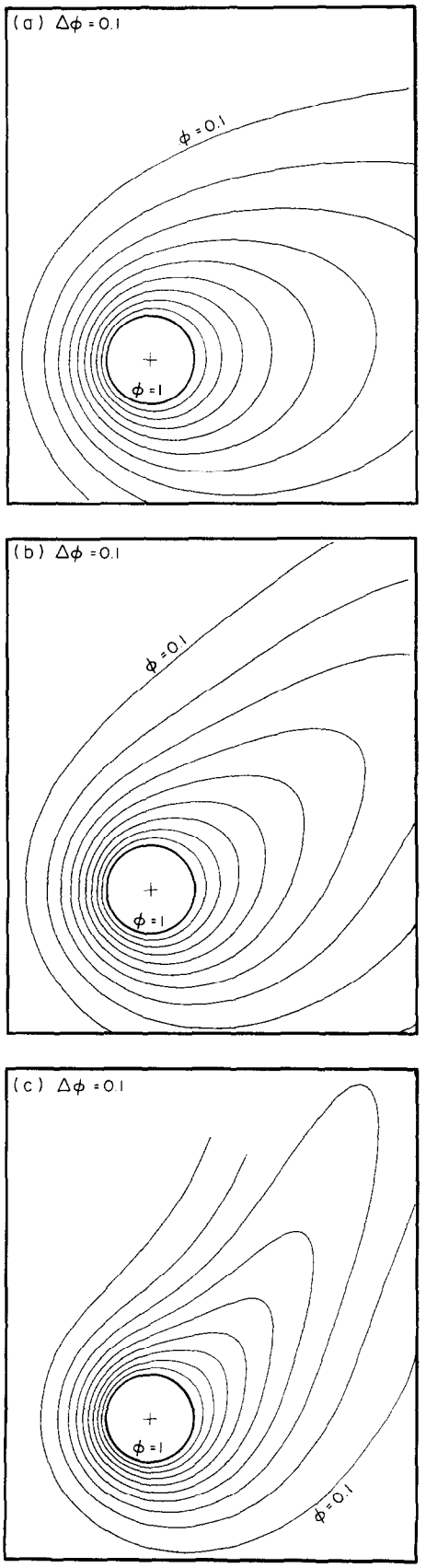

FIG. 10. Isotherms for $Re = 5$. (a) $Gr = 5$. (b) $Gr = 30$. (c) $Gr = 100$.

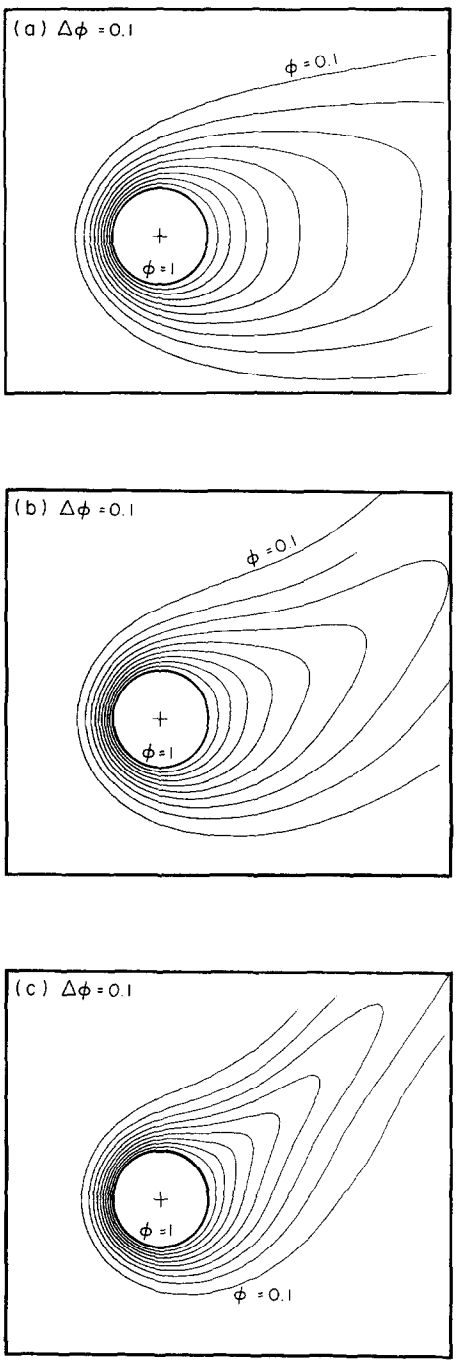

FIG. 11. Isotherms for the cases of $Re = 20$. (a) $Gr = 100$. (b) $Gr = 500$. (c) $Gr = 2000$.

REFERENCES

1. S. C. R. Dennis, J. D. Hudson and N. Smith, Steady laminar forced convection from a circular cylinder at low Reynolds numbers, *Physics Fluids* **11**, 933–940 (1967).
2. S. Nakai and T. Okazaki, Heat transfer from a horizontal circular wire at small Reynolds and Grashof numbers – I, *Int. J. Heat Mass Transfer* **18**, 387–396 (1975).
3. T. H. Kuehn and R. J. Goldstein, Numerical solution to the Navier–Stokes equations for laminar natural convection about a horizontal isothermal circular cylinder, *Int. J. Heat Mass Transfer* **23**, 971–979 (1980).
4. B. Farouk and S. I. Guceri, Natural convection from a horizontal cylinder—Laminar regime, *J. Heat Transfer* **103**, 522–527 (1981).
5. S. Nakai and T. Okazaki, Heat transfer from a horizontal circular wire at small Reynolds and Grashof numbers—II, *Int. J. Heat Mass Transfer* **18**, 397–413 (1975).
6. D. C. Collis and M. J. Williams, Two-dimensional convection from heated wires at low Reynolds numbers, *J. Fluid Mech.* **6**, 357–384 (1959).
7. A. P. Hatton, D. D. James and H. W. Swire, Combined forced and natural convection with low-speed air flow over horizontal cylinders, *J. Fluid Mech.* **42**, 17–31 (1970).
8. B. Gebhart and L. Pera, Mixed convection for long horizontal cylinders, *J. Fluid Mech.* **45**, 49–64 (1970).
9. G. K. Sharma and S. P. Sukhatme, Combined free and forced convection heat transfer from a heated tube to a transverse air stream, *J. Heat Transfer* **91**, 457–459 (1969).
10. R. M. Fand and K. K. Keswani, Combined natural and forced convection heat transfer from horizontal cylinders to water, *Int. J. Heat Mass Transfer* **16**, 1175–1191 (1973).
11. W. D. Bennon and F. P. Incropera, Mixed convection heat transfer from horizontal cylinders in the cross flow of a finite water layer, *J. Heat Transfer* **103**, 540–545 (1981).
12. P. H. Oosthuizen and S. Madan, The effect of flow direction on combined convective heat transfer from cylinders to air, *J. Heat Transfer* **93**, 240–242 (1971).
13. P. H. Oosthuizen and S. Madan, Combined convection heat transfer from horizontal cylinders in air, *J. Heat Transfer* **92**, 194–196 (1970).
14. T. W. Jackson and H. H. Yen, Combined forced and free convective equations to represent combined heat-transfer coefficients for horizontal cylinders, *J. Heat Transfer* **93**, 247–248 (1971).
15. A. Acrivos, On the combined effect of forced and free convection heat transfer in laminar boundary layer flows, *Chem. Engng Sci.* **21**, 343–352 (1966).
16. E. M. Sparrow and L. Lee, Analysis of mixed convection about a horizontal cylinder, *Int. J. Heat Mass Transfer* **19**, 229–232 (1976).
17. J. H. Merkin, Mixed convection from a horizontal circular cylinder, *Int. J. Heat Mass Transfer* **20**, 73–77 (1976).
18. J. O. Wilkes and S. W. Churchill, The finite-difference computation of natural convection in a rectangular enclosure, *A.I.Ch.E. Jl* **12**, 161–166 (1966).
19. W. M. Collins and S. C. R. Dennis, Flow past an impulsively started circular cylinder, *J. Fluid Mech.* **60**, 105–127 (1973).
20. H. M. Badr and S. C. R. Dennis, Unsteady flow past a rotating and translating circular cylinder, *Proc. 8th Canadian Congr. Applied Mechanics*, pp. 659–660 (1981).
21. S. C. R. Dennis and G. Chang, Numerical integration of the Navier–Stokes equations in two-dimensions, Math. Research Center, U.S. Army, Tech. Rep. No. 859 (1969).

APPENDIX

The functions S_0, S_{n1} and S_{n2} used in equations (16a), (16b) and (16c) are defined as

$$S_0(\xi,t) = e^{\xi}\frac{Gr}{2Re^2}\left(\frac{\partial H_1}{\partial \xi} + H_1\right) + \sum_{n=1}^{N} n\left(F_n\frac{\partial g_n}{\partial \xi} - f_n\frac{\partial G_n}{\partial \xi} + g_n\frac{\partial F_n}{\partial \xi} - G_n\frac{\partial f_n}{\partial \xi}\right), \quad \text{(A1)}$$

$$S_{n1}(\xi,t) = e^{\xi}\left(\frac{Gr}{2Re^2}\right)\left[\frac{\partial h_{n-1}}{\partial \xi} + \frac{\partial h_{n+1}}{\partial \xi} - (n-1)h_{n-1} + (n+1)h_{n+1}\right] + \sum_{m=1}^{N}\left\{\frac{\partial g_m}{\partial \xi}(Kf_K - Jf_J) + \frac{\partial G_m}{\partial \xi}[KF_K - (m-n)F_J] + mg_m\left[\frac{\partial f_K}{\partial \xi} - \operatorname{sgn}(m-n)\frac{\partial f_J}{\partial \xi}\right] + mG_m\left(\frac{\partial F_K}{\partial \xi} - \frac{\partial F_J}{\partial \xi}\right)\right\}, \quad \text{(A2)}$$

$$S_{n2}(\xi,t) = e^{\xi}\left(\frac{Gr}{2Re^2}\right)\left[\delta_n\frac{\partial H_0}{\partial \xi} + \frac{\partial H_{n-1}}{\partial \xi} + \frac{\partial H_{n+1}}{\partial \xi} + (n+1)H_{n+1} - (n-1)H_{n-1}\right] + \sum_{m=1}^{N}\left\{\frac{\partial g_m}{\partial \xi}[KF_K + (m-n)F_J] - \frac{\partial G_m}{\partial \xi}(Kf_K + Jf_J) + mg_m\left(\frac{\partial F_K}{\partial \xi} + \frac{\partial F_J}{\partial \xi}\right) - mG_m\left[\frac{\partial f_K}{\partial \xi} + \operatorname{sgn}(m-n)\frac{\partial f_J}{\partial \xi}\right]\right\} \quad \text{(A3)}$$

where

$$K = m+n, \quad J = |m-n|, \quad \delta_n = \begin{cases} 1 \text{ when } n = 1 \\ 0 \text{ when } n \neq 1 \end{cases}$$

and $\operatorname{sgn}(m-n)$ means the sign of the term $(m-n)$. All functions with subscripts less than 1 or more than N should be equated to zero.

The definitions of the functions Z_0, Z_{n1} and Z_{n2} used in equations (17a), (17b) and (17c) are as follows:

$$Z_0(\xi,t) = \sum_{n=1}^{N} n\left(F_n\frac{\partial h_n}{\partial \xi} - f_n\frac{\partial H_n}{\partial \xi} + h_n\frac{\partial F_n}{\partial \xi} - H_n\frac{\partial f_n}{\partial \xi}\right), \quad \text{(A4)}$$

$$Z_{n1}(\xi,t) = \sum_{m=1}^{N}\left\{\frac{\partial h_m}{\partial \xi}(Kf_K - Jf_J) + \frac{\partial H_m}{\partial \xi}[KF_K - (m-n)F_J] + mh_m\left[\frac{\partial f_K}{\partial \xi} - \operatorname{sgn}(m-n)\frac{\partial F_J}{\partial \xi}\right] + mH_m\left(\frac{\partial F_K}{\partial \xi} - \frac{\partial F_J}{\partial \xi}\right)\right\}, \quad \text{(A5)}$$

$$Z_{n2}(\xi,t) = \sum_{m=1}^{N}\left\{\frac{\partial h_m}{\partial \xi}[KF_K + (m-n)F_J] - \frac{\partial H_m}{\partial \xi}(Kf_K + Jf_J + mh_m\left(\frac{\partial F_K}{\partial \xi} + \frac{\partial F_J}{\partial \xi}\right) - mH_m\left[\frac{\partial f_K}{\partial \xi} + \operatorname{sgn}(m-n)\frac{\partial f_J}{\partial \xi}\right]\right\}. \quad \text{(A6)}$$

ETUDE THEORIQUE DE LA CONVECTION LAMINAIRE MIXTE AUTOUR D'UN CYLINDRE HORIZONTAL DANS UN ECOULEMENT FRONTAL

Résumé—On considère le problème de la convection laminaire mixte autour d'un cylindre isotherme horizontal. La direction de l'écoulement est horizontale et perpendiculaire à l'axe du cylindre. L'étude est basée sur la résolution de l'équation complète de Navier–Stokes, et de celle de l'énergie pour un écoulement bidimensionnel de fluide de Boussinesq. L'écoulement est supposé partir brusquement du repos et les couches limites dynamique et thermique se développent dans le temps jusqu'à atteindre les conditions permanentes. L'étude couvre les domaines de nombres de Reynolds $1 < Re < 40$ et de Grashof jusqu'à $Gr = 5\,Re^2$, tandis que le nombre de Prandtl est maintenu à 0,7. La comparaison des résultats avec des données expérimentales antérieures montre un bon accord. Les configurations de lignes de courant et d'isothermes sont dessinées et on discute différents aspects du phénomène.

THEORETISCHE UNTERSUCHUNG DER LAMINAREN GEMISCHTEN KONVEKTION AN EINEM WAAGERECHTEN, QUER ANGESTRÖMTEN ZYLINDER

Zusammenfassung—Das Problem der laminaren gemischten Konvektion an einem waagerechten isothermen Zylinder wird betrachtet. Die Richtung des freien Stroms wird horizontal und im rechten Winkel zur Zylinderachse angenommen. Die Untersuchung basiert auf der Lösung der vollständigen Navier–Stokes- und Energiegleichungen für die zweidimensionale Strömung eines Boussinesq-Fluids. Es wird angenommen, daß der freie Strom plötzlich aus dem Ruhezustand anläuft und sich Geschwindigkeits- und thermische Grenzschichten mit der Zeit bis zum stationären Zustand entwickeln. Die Untersuchung erstreckt sich über einen Bereich der Reynolds-Zahl von $Re = 1$ bis $Re = 40$ und bis zu Grashof-Zahlen von $Gr = 5\,Re^2$, während die Prandtl-Zahl auf dem konstanten Wert von $Pr = 0{,}7$ gehalten wird. Der Vergleich mit früheren experimentellen Beziehungen zeigt gute Übereinstimmung. Stromlinien und Isothermen werden dargestellt und verschiedene Aspekte des Vorgangs diskutiert.

ТЕОРЕТИЧЕСКОЕ ИССЛЕДОВАНИЕ ЛАМИНАРНОЙ СМЕШАННОЙ КОНВЕКЦИИ ОТ ПОПЕРЕЧНО ОБТЕКАЕМОГО ГОРИЗОНТАЛЬНОГО ЦИЛИНДРА

Аннотация — Рассмотрена задача о ламинарной смешанной конвекции от горизонтального изотермического цилиндра. Предполагается, что свободный поток направлен горизонтально и перпендикулярно к оси цилиндра. Исследование проводится на основе решения полных уравнений Навье-Стокса и энергии для двумерного течения жидкости в приближении Буссинеска. Предполагается, что свободное течение начинается внезапно из состояния покоя, а динамические и тепловые пограничные слои развиваются со временем вплоть до установления стационарного режима. Исследование проводится в диапазоне изменения числа Рейнольдса $1 < Re < 40$ при значении числа Грасгофа, равном $Gr = 5 \times 10^2$, и постоянном значении числа Прандтля, равном 0,7. Результаты хорошо описывают ранее полученные экспериментальные зависимости. Представлены графики линий тока и изотерм и рассмотрены различные аспекты процесса.